Journal of Scientific & Industrial Research
Vol. 83, January 2024, pp. 5-14
DOI: 10.56042/jsir.v83i1.2580

Surface Modification of Al-7075 Alloy by SiC-Cu Ceramic Electrode in Electrical Discharge Coating

Lokesh Kumar Ranjan[1], Sujoy Chakraborty[1]*, Uttam Kumar Mandal[1], Siddhartha Kar[2] & Arabinda Meher[3]

[1]Department of Production Engineering, National Institute of Technology Agartala, Tripura 799 046, India
[2]Department of Industrial Engineering & Management, M S Ramaiah Institute of Technology, Bangalore 560 054, India
[3]Department of Research & Development, Chandigarh University, Mohali 140 413, India

Received 12 June 2023; revised 20 November 2023; accepted 28 December 2023

The present study aims to enhance and evaluate Electrical Discharge Coating (EDC) on Al-7075 alloy using SiC-Cu ceramic electrode. The study analyses the impact of input parameters such as current, composition and compaction load on EDC responses, including Material Deposition Rate (MDR), Tool Wear Rate (TWR) and Surface Roughness (SR). Trial tests were performed using Taguchi's L9 experimental design, and thereafter, Grey Relational Analysis (GRA) and technique for order preference by similarity to an ideal solution (TOPSIS) were implemented to optimize all the responses. The experiments were optimized to achieve a higher MDR, lower TWR and lower SR. Analysis of variance was also employed to statistically investigate the experimental data and determine the contribution of each parameter to achieve better results. Optimum condition was achieved with a compaction load of 5 ton, current 6 A and composition 50:50, using both the GRA and TOPSIS methods. At the optimum condition, there was an improvement in GRA from 0.5603 to 0.7778, while TOPSIS showed an improvement from 0.2418 to 0.7659. Further, the morphology of the coated surface was investigated using scanning electron microscopy images and X-ray diffraction analyses, which confirmed the migration of SiC-Cu from the tool materials.

Keywords: Coating, Electrical discharge coating, Grey relational analysis, Silicon carbide, TOPSIS

Introduction

The rigidity of machined parts is essential in engineering applications because surface breakdown can occur when these components are exposed to extreme conditions, such as high temperatures and critical corrosion conditions. Thus, it is essential to extend the surface properties of the material along with its mechanical properties. Traditional methods for improving surface qualities, such as ion implantation, plasma arc spraying, and deposition by chemical vapour or physical vapour processes, involve expensive equipment and present challenging experimental circumstances.[1] In recent years the use of Electrical Discharge Machining (EDM) has become a viable option for surface modification.[2,3] EDM is a novel machining process for cutting challenging materials, wherein the process is unaffected by the hardness of the work piece material but should be electrically conductive.[4,5] EDM is employed in many fields including aerospace, automotive, microelectronics, bioengineering, and die and mold manufacturing.[6] In EDM, electric sparks are generated between the work piece and the tool electrodes in a liquid dielectric environment. These electrical discharges produce temperatures higher than the melting point of the electrodes at the point of discharge. The electrodes are melted and vaporized by the EDM process.[7,8] Erosion removes material from both the electrodes, leaving tiny craters on the surfaces of the tool and workpiece.[9,10] A portion of the molten material re-solidifies at the base of the crater and forms a white layer on the surface, leading to the concept of Electrical Discharge Coating (EDC).

Powder metallurgy (P/M) electrodes and traditional electrodes can be employed to alter the machined surface.[11] Chakraborty *et al.*[12] reviewed the phenomenon of surface alteration by EDC, which involves deposition of material by the P/M tool to the substrate to improve its surface. In this method, tool electrodes are fabricated using powder materials like TiC, WC, Ti, Ta, Cu, and Cr. These P/M electrodes exhibit a significantly different influence on responses such as tool wear and transfer of material compared to other common electrodes. P/M tools are more susceptible to breakage from spark discharges

*Author for Correspondence
E-mail: ersujoymech05@gmail.com

compared to the conventional electrodes. They also offer the flexibility of being mixed in varying proportions and compacted under different load conditions.[13] All the aforementioned factors contribute to the formation of a dense white layer but are also associated with an increased susceptibility to defects such as micro-cracking. Moreover, P/M tools are scientifically feasible for EDM processes, facilitating the integration of desirable material properties. Electrode performance is influenced by P/M parameters such as sintering temperature and compacting pressure.[14] Since the powder particles have a weak bond, P/M green tools are employed to transfer the desired material for forming a film on the substrate surface.

The modification of surfaces using EDC with sintered and green P/M tools is a contentious topic in scientific research.[15–17] Patowari *et al*.[18] investigated the surface integrity of C-40 steel in EDM with green compact WC-Cu P/M tool. They evaluated the material deposition rate (MDR), Tool Wear Rate (TWR), and Surface Roughness (SR) as the output parameters. WC was found to be deposited on the work surface in a firm and homogeneous layer. The results were significantly influenced by both pulse on-time (T_{on}) and current. Gill & Kumar[19] used Cu-Mn P/M electrodes to machine a hot die steel (H_{11}). The increase in micro hardness values was attributed to the formation of cementite, along with phases of ferrite and manganese carbide. Gulcan *et al*.[20] analyzed the impact of Cu-Cr and Cu-Mo P/M tools on SAE 1040 steel work piece. They observed improvements in the micro hardness, corrosion resistance, and abrasion resistance of the machined surfaces compared to the base material. Kumar *et al*.[21] deposited a hard composite layer on OHNS steel using Cu-CrB_2 P/M tool in EDM. Chundru *et al*.[22] employed TiC/Cu P/M tool with powder sizes ranging from nano to micron levels to modify the surface of Ti6Al4V alloy through EDM. It was found that nanopowder tools resulted in significantly higher surface alloying compared to other tools, attributable to their elevated reactive surface area. Mazarbhuiya and Rahang[23] utilized W75%–Cu25% P/M green compact tool to execute selective area deposition on Al-6061 alloy through EDM. The micro hardness of the modified surface showed a 3.3 times improvement compared to the base material. Sarmah *et al*.[24] conducted EDC experiments for modifying the surface of Al-7075 using Inconel-Al P/M tools. They observed that the MDR decreased with an increase in T_{on}, while it increased with an increase in current up to a critical limit, beyond which it decreased. The deposited layer exhibited micro hardness 1.5–2.5 times greater than that of the base material. Several studies on EDM have investigated the influence of parameters on work piece and tool wear, geometrical characteristics, and accuracy. The literature survey reveals that process parameters play a crucial role in both machining and coating processes. Hence, identifying the optimal combination of process parameters is essential for achieving better results. Researchers have also used various optimization techniques to improve various EDM parameters.[17,25–27] Some research papers have employed the Taguchi method with analysis of variance (ANOVA) to identify optimum conditions and assess the significance of individual process parameters.[8,28,29] For simultaneous optimization of multiple responses, the technique for order preference by similarity to an ideal solution (TOPSIS) has been profoundly used in EDM domain.[17,26]

The present study analyzes the deposition of tool material made from a mixture of silicon carbide (SiC) and copper (Cu) onto the Al-7075 substrate using EDC process, with a focus on process parameter optimization to obtain better results. Al-7075 alloy is widely utilized in the aviation, marine and automobile sectors. The deposition of this mixture onto the Al-7075 alloy makes it suitable for use in high-temperature and hostile situations. Based on contemporary literature, no articles have been reported on improving the surface properties of Al-7075 using the EDC process with SiC-Cu green compacted electrodes. Moreover, grey relational analysis (GRA) and TOPSIS are used in this study to optimize the process parameters, while ANOVA is used to analyze the most significant influencing parameters. The combination of GRA and TOPSIS is a new hybrid optimization concept not utilized in any article for EDC process parameter optimization, and the EDC process is also not yet industrialized. Thus, there is still scope for further research. The experimental investigation and optimization of process parameters for coating SiC-Cu on Al-7075 are explained in detail below.

Materials and Methods

Materials Used and Experimental Setup

The tool electrodes were fabricated using the P/M method and consisted of SiC and Cu powders. In the present study, three levels of SiC and Cu powder

mixtures- 30:70, 40:60 and 50:50-were utilized. Here, Cu serves as both a binder and conductive fabric, thereby enhancing the tool conductivity. The mixture was prepared by grinding with a pestle and mortar for one hour to obtain the desired combination. Each resulting powder mixture was then compacted at three different loads (5, 10 and 15 ton) in a pellet press to obtain the final shape of 13 mm diameter and 2.5 mm thickness. Thereafter, the pellets were glued to Cu extensions using a conductive paste, forming the final tool electrode.

A die-sinking EDM (Spark on ix F25) with a servo head, dielectric tank, pump, and control unit was employed for experiments (Fig. 1). The servo head in EDM ensures a consistent separation between the tool and work piece during the experiment. The substrate material chosen was Al-7075 alloy, part of the 7xxx series of aluminium alloys that utilize zinc and magnesium as primary alloying elements. The elemental arrangement of the work piece is presented in Table 1. The work piece used in this study had dimensions of 13 × 13 × 5 mm.

The variable parameters for this work, namely compaction load, current, and composition, significantly impact the EDC process. Numerous trials were conducted on the work surface of Al-7075 alloy with SiC-Cu P/M tool and EDM oil as the dielectric. Among the EDM parameters, current impacted the outcome of the EDC experiments significantly. So, current was varied at three levels, ranging from 2 to 6 A. The duty cycle was kept constant at 50% throughout the experiments, and the machining time was fixed at 4 minutes. A gap voltage of 55–60 V was consistently maintained. Machining and deposition occur concurrently in the EDC process. To facilitate the deposition of tool material on the work piece surface, the tool and work piece were connected with reverse polarity. The ranges of input variables along with their respective levels are presented in Table 2, while the L9 orthogonal arrays with three responses for each set of experiments are presented in Table 3.

To obtain the values of MDR and TWR, the weight of the work piece and tool before and after the experiment was measured using a precise weighing balance device. The Eqs (1 & 2) were used to compute the MDR and TWR.

$$\text{MDR} = \frac{\begin{matrix}Weight\ of\ wrok\ piece\ after\ experiment-\\ Weight\ of\ work\ piece\ before\ experiment\end{matrix}}{Time\ of\ experiment} mg/min \quad \ldots (1)$$

$$\text{TWR} = \frac{\begin{matrix}Weight\ of\ tool\ before\ \ experiment\ -\\ Weight\ of\ tool\ after\ \ experiment\end{matrix}}{Time\ \ of\ \ experiment} mg/min \quad \ldots (2)$$

The SR of the coated samples was measured using a surface profilometer (Make: Mitutoyo Surftest; Model: SV-514). In the current study, the centre-line average roughness, i.e., Ra, was considered as the SR parameter. It calculates the arithmetic average of the profile departure from the mean line.[30]

The coated samples were analyzed by scanning electron microscopy (SEM) and X-ray diffraction (XRD) to characterize the surfaces obtained after coating and to check the phases formed by the coating.

Fig. 1 — Die-sink EDM (Sparkonix F25)

Table 2 — Variables and their levels for Taguchi L9 orthogonal array

Variables	Unit	Level 1	Level 2	Level 3
Compaction Load	ton	5	10	15
Current	ampere	2	4	6
Composition	percentage	30:70	40:60	50:50

Table 1 — The elemental composition of Al-7075 alloy

Elements	Cr	Mn	Cu	Fe	Mg	Si	Ti	Zn	Al
Composition (%)	0.2	0.3	2	0.5	2.9	0.4	0.2	6.1	Remaining

Table 3 — Observation table

Run order	*Compaction load (ton)*	*Current (Ampere)*	*Composition (SiC:Cu)*	*MDR (mg/min)*	*TWR (mg/min)*	*Ra (μm)*
1	5	2	30:70	0.124	4.3793	2.101
2	5	4	40:60	0.150	4.6620	2.565
3	5	6	50:50	0.385	13.6509	3.701
4	10	2	40:60	0.210	7.5015	2.794
5	10	4	50:50	0.177	5.7102	2.864
6	10	6	30:70	0.171	5.2240	2.671
7	15	2	50:50	0.107	4.9988	2.626
8	15	4	30:70	0.166	7.4317	2.908
9	15	6	40:60	0.215	5.7759	2.614

Table 4 — GRG preference values with their respective ranks

Run	*Normalized value*			*Grey relation coefficient*			*GRG*	*Rank*
	MDR	*TWR*	*SR*	*MDR*	*TWR*	*SR*		
1	0.0612	0.0000	1.0000	0.3475	0.3333	1.0000	0.5603	2
2	0.1547	0.0305	0.7100	0.3717	0.3402	0.6329	0.4483	5
3	1.0000	1.0000	0.0000	1.0000	1.0000	0.3333	0.7778	1
4	0.3705	0.3367	0.5669	0.4427	0.4298	0.5358	0.4694	4
5	0.2518	0.1435	0.5231	0.4006	0.3686	0.5118	0.4270	9
6	0.2302	0.0911	0.6438	0.3938	0.3549	0.5839	0.4442	6
7	0.0000	0.0668	0.6719	0.3333	0.3489	0.6038	0.4287	8
8	0.2122	0.3292	0.4956	0.3883	0.4271	0.4978	0.4377	7
9	0.3885	0.1506	0.6794	0.4498	0.3705	0.6093	0.4766	3

Methodologies

GRA and TOPSIS methods were used in the present study to select the best parametric combination from a set of different input parameters such as compaction load, current, and composition.

Taguchi Method

The Taguchi method is effective in reducing the number of runs required to identify the parametric effects on the responses. The benefit of using this system lies in its ability to save time and effort in conducting experiments and determining optimal parametric combination.[31] In this study, Taguchi L9 orthogonal array, is framed, providing a structured combination of process parameters, based on which the experiments are performed.

Grey Relational Analysis

Nowadays, engineering problems involve multi-response issues that can be consolidated into a single objective problem. The GRA method is widely used for reducing multi-objective problems into a singular objective. This technique establishes a relationship between a system, its uncertainties, real data correlation values and performance using Grey Relational Grade (GRG). The solution is provided by the higher-grade value, wherein GRA transforms all performance characteristics into a singular GRG.[25,27] Moreover, this technique allows the examination of multiple aspects with a small amount of data. The following steps were taken to convert the multi-response to a unique GRG.

Step-1: After getting the observed values of the responses, these values were normalized using Eqs (3 & 4).

$$\text{Larger the better } N_i^*(k) = \frac{y_i(k) - min\ y_i(k)}{max\ y_i(k) - min\ y_i(k)} \quad \ldots (3)$$

$$\text{Smaller the better } N_i^*(k) = \frac{max\ y_i(k) - y_i(k)}{max\ y_i(k) - min\ y_i(k)} \quad \ldots (4)$$

where, $i = 1, 2, 3,\ldots,$m; $k = 1, 2, 3,\ldots,$ n, $m =$ number of trials, $n =$number of factors, $y_i(k) =$ original sequence, $N_i^*(k) =$ normalized value, $\min y_i(k) =$ minimum value of $y_i(k)$ and $\max y_i(k) =$ maximum value of $y_i(k)$.The final normalized values for the response are given in the Table 4.

Step-2: The grey relational coefficient (GRC) was subsequently estimated by Eq. (5) to ascertain the association between the ideal and the normalized values of the experiment.

$$\varepsilon_i(k) = \frac{\Delta_{\min} + \tau\Delta_{\max}}{\Delta_{0i}(k) + \tau\Delta_{\max}} \quad \ldots (5)$$

where, $\varepsilon_i(k) = \text{GRC}, \Delta_{0i} =$ deviation among $N_o^*(k)$ and $N_i^*(k)$, $N_o^*(k) =$ ideal sequence, $\Delta_{max} =$ maximum value of $\Delta_{0i}(k), \Delta_{min} =$ minimum value of $\Delta_{0i}(k), \tau =$ distinguishing coefficient. In the present study, τ was taken as 0.5.

Step-3: At this phase, the final GRG was calculated by taking the average of all the GRC values as per Eq. (6).

$$\text{Grey relational grade, } GRG = \frac{1}{m}\sum \varepsilon_i\,(k) \quad \ldots (6)$$

where, $m =$ total number of responses.The higher value of GRG denotes a better degree of correlation between the current series and the ideal series. The ideal series is the optimal response in practice. Also, the highest value of GRG denotes the optimal value of the reaction of the system.

Step-4: The GRG values are then ranked in descending order as shown in Table 4.

Technique for Order of Preference by Similarity to Ideal Solution

To address multi-objective situations, TOPSIS had been widely employed due to its utilization of the minimum and maximum distances from the ideal result theory.[32] TOPSIS is a popular and widely used multi-criteria decision making method for material selection, location, network, site selection, and machining parameter selection.[26] In this approach, the following steps were followed.

Step-1: In the first step, the following formula, as shown in Eq. (7), was used to normalize the data.

$$R_{ij} = X_{ij} / \sum X_{ij}^2 \quad \ldots (7)$$

where, $i = 1, 2, 3, \ldots, m; j = 1, 2, 3, \ldots, n$

Step-2: In this step, weights were assigned to each criterion. All input parameters were given an equal percentage of weights in the present study.

Step-3: In this step, a matrix with normalized weights was created, where each column of the normalized matrix was multiplied by the individual weights as per Eq. (8).

$$V_{ij} = W_j \times R_{ij} \quad \ldots (8)$$

where, $j = 1, 2, \ldots, n$ and W_j represents weight of the variables. In the present study weightages of 0.333, 0.333 and 0.334 were assigned to MDR, TWR and SR, respectively. The weighted normalized matrices for the output responses are displayed in Table 5.

Step-4: This step uses the following Eqs. (9) and (10) to find the positive ideal solution (PIS) and negative ideal solution (NIS), respectively.

$$\text{PIS, } A^+ = \{V_1^+, \ldots, V_n^+\} \quad \ldots (9)$$

where, $V_j^+ = \{max(V_{ij})ifj \in J, min(V_{ij})ifj \in J'\}$

$$\text{NIS, } A^- = \{V_1^-, \ldots, V_n^-\} \quad \ldots (10)$$

where, $V_j^- = \{min(V_{ij})ifj \in J, max(V_{ij})ifj \in J'\}$. The PIS and NIS are displayed in Table 5.

Step-5: The separation measures from the ideal alternative (S^+) and non-idealalternative (S^-) were calculated using the Eqs. (11) and (12) between the PIS and NIS.

$$S_i^+ = \left[\sum (V_j^+ - V_{ij})^2\right]^{1/2} \quad \ldots (11)$$

$$S_i^- = \left[\sum (V_j^- - V_{ij})^2\right]^{1/2} \quad \ldots (12)$$

where, $i = 1, 2, 3, \ldots, m$ and $j = 1, 2, 3, \ldots, n$.

Step-6: For each alternative, relative closeness (P_i) was found using Eq. (13).

Table 5 — TOPSIS preference values with their respective ranks

Run	*Weighted Normalized Value*			*Separation Measure*		*Preference*	*Rank*
	MDR	*TWR*	*SR*	S_i^+	S_i^-	P_i	
1	0.067	0.068	0.083	0.201	0.064	0.241	6
2	0.081	0.072	0.101	0.189	0.051	0.212	8
3	0.207	0.211	0.146	0.063	0.207	0.766	1
4	0.113	0.116	0.110	0.136	0.082	0.374	2
5	0.095	0.088	0.113	0.169	0.054	0.243	5
6	0.092	0.081	0.105	0.175	0.055	0.238	7
7	0.058	0.077	0.104	0.202	0.043	0.177	9
8	0.089	0.115	0.115	0.155	0.065	0.295	4
9	0.116	0.089	0.103	0.153	0.075	0.329	3

$$P_i = \frac{S_i^-}{(S_i^+ + S_i^-)} \quad \ldots (13)$$

In this regard, higher P_i was preferable.

Results and Discussions

A total of nine experiments were successfully carried out based on the L9 orthogonal array. This experimental investigation yielded a wide range of MDR (0.107 – 0.385 mg/min), TWR (4.379 – 13.651 mg/min) and SR (2.101 – 3.701 µm). A comprehensive discussion of the results obtained is presented herein.

Effects of Process Parameters on the Responses

The values of MDR, TWR and SR are presented in Table 3. Considering composition as an input variable, Fig. 2a illustrates that MDR is lower for electrodes with a higher composition of binding material, i.e., Cu. This can be attributed to the higher binding capacity and thermal conductivity of Cu. As a result, a higher Cu ratio (i.e., with 70%) limits the faster transfer of the tool material over the substrate surface. It is also clear that MDR acts inversely with a rise in compaction load. The MDR is higher at lower compaction loads, such as 5 ton, and the MDR decreases as the load increases. Elsewhere, an increase in MDR is observed with increasing current from 2 to 6 A. During the experiments, the highest MDR is observed at a current of 6 A, attributed to the increased intensity of the spark at higher current. Hence, the optimal parameter setting in this case has been found in the combination of 1-3-3, which indicates that the compaction load is 5 ton, the current setting is 6 A, and the tool composition is 50:50.

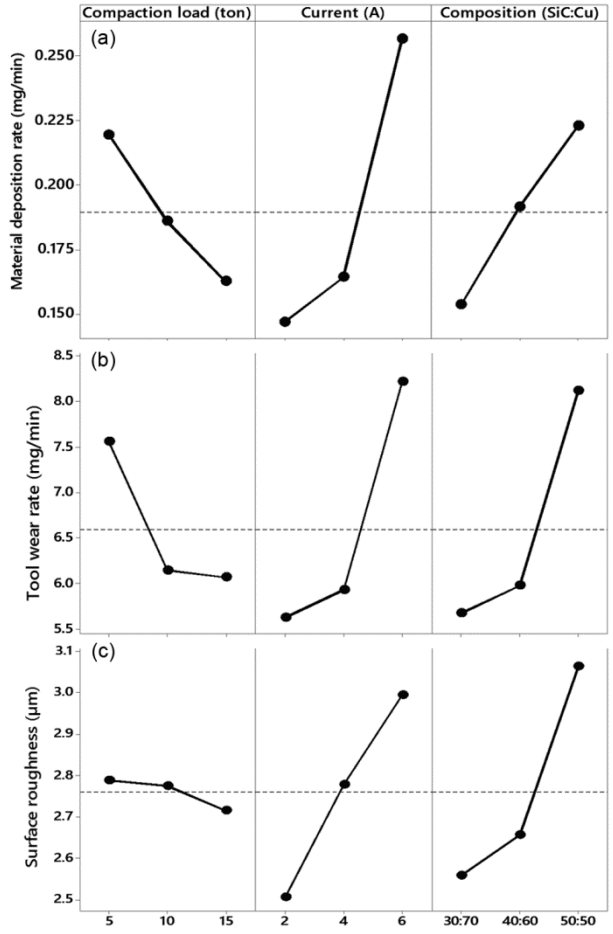

Fig. 2 — The effect of variables on: (a) material deposition rate; (b) tool wear rate; and (c) surface roughness

Similarly, Fig. 2b shows that the highest TWR occurs at lower compaction load and it decreases as the load increases. The bonding strength combined with the composition is crucial in this case. Tool wear is more for tools with less binding material (Cu) and increases as the composition of the binding material decreases. Consequently, a higher binding material ratio prevents more tool material erosion during EDC. There is an increase in TWR at a higher level of current and composition. As the current increases, the discharge intensity increases, resulting in more tool material erosion. Here, the optimal parameter setting has been found in the combination of 3-1-1, which indicates that the compaction load is 15 ton, the current setting is 2 A, and the tool composition is 30:70.

The mean parametric effect of the process parameters on SR is displayed in Fig. 2c. The SR decreases with an increase in the compaction load. The tool becomes denser with increased compaction load, which leads to less tool wear and subsequently less material deposition.[15] This situation leads to a lower SR of the deposition. SR increases with an increase in current, which can be attributed to the bigger and deeper craters formed on the coated surface. The increase in the intensity of spark with increased current is responsible for the increment in the size of the craters. It might also be noted that the SR increases with a rise in the percentage of SiC in the composition of tools. This is primarily due to increased tool material deposition and crater formation on the work surface. Hence, the optimal parameter setting in this case has also been found in the combination of 3-1-1, which indicates that the compaction load is 15 ton, the current setting is 2 A, and the tool composition is 30:70.

Analysis of GRA and TOPSIS

Both GRA and TOPSIS were calculated using equations 3 to 6 and equations 7 to 13, respectively.

The GRG values and TOPSIS preference values (P_i) along with their corresponding rankings in descending order are presented in Tables 4 and 5, respectively. From GRG, run 3 evolved as the highest rank followed by run 1 and run 9. Similarly, for TOPSIS, run 3 evolved as the highest rank followed by run 4 and run 9. Thus, the parametric combination for run 3 appears to be the optimal setting in both the analysis for the responses. Further, the significance of the process parameters in both the GRA and TOPSIS methods are also assessed using the ANOVA technique. The mean response for GRG and TOPSIS is displayed in Table 6, whereas the ANOVA results for the GRG and TOPSIS are presented in Table 7. It has been noticed that compaction load is the most important factor contributing the most, followed by current and composition for GRA. For TOPSIS, the most important factor is current, followed by compaction load and composition.

Confirmatory Experiment with GRA and TOPSIS

Confirmatory experiments were conducted, and the results presented in Table 8 indicate that GRA improved by 0.2175 from the initial run to the optimal run, while TOPSIS improved by 0.5241, respectively.

Surface Morphology

The coating surface at optimal condition (run 3: 5 ton, 6 A and 50:50) was characterized by the SEM analysis, as shown in Fig. 3a. From the figure, it is clear that the transfer of tool material takes place on the base material which is separated by an area of interface. The base material, deposited material, and interface is also visible in Fig. 3a. Further examination of the sample also confirmed that the transfer of tool material occurred on the work surface and accumulated in the form of agglomerates as shown in Fig. 3b. This image also reveals that a SiC like particle is visible on the surface of the substrate. From the SEM analysis of the initial condition (run 1: 5 ton, 2 A, 30:70), it is found that crater formation takes place on the work surface, as shown in Fig. 3c, which may be due to the increase in T_{on}.

Furthermore, for layer thickness analysis, the cross-section of the polished surface was etched in Keller solution for 1 minute to reveal the deposited layer

Table 6 — Means response table for GRG

Level	*Compaction load (ton)*	*Current (Ampere)*	*Composition (SiC:Cu)*
	A. GRG		
1	0.595	0.486	0.481
2	0.447	0.438	0.465
3	0.448	0.566	0.544
Delta	0.149	0.129	0.080
Rank	1	2	3
	B. TOPSIS		
1	0.407	0.265	0.258
2	0.285	0.250	0.305
3	0.267	0.445	0.396
Delta	0.139	0.195	0.137
Rank	2	1	3

Table 8 — GRA and TOPSIS experimental outcomes

Variables	*Initial set*	*Optimal set*
Levels	1-1-1	1-3-3
Compaction Load	5	5
Current	2	6
Composition	30:70	50:50
MDR	0.124	0.385
TWR	4.3793	13.6509
Ra	2.101	3.701
GRG value	0.5603	0.7778
TOPSIS (P_i) value	0.2418	0.7659
Enhancement in GRG	—	0.2175
Enhancement in TOPSIS	—	0.5241

Table 7 — ANOVA for GRG and TOPSIS

Source	*DF*	*Seq SS*	*Contribution*	*Adj SS*	*Adj MS*	*F-Value*	*P-Value*
A. GRG							
Compaction load (ton)	2	0.044	42.94%	0.044	0.022	1.96	0.338
Current (A)	2	0.025	24.71%	0.025	0.013	1.13	0.470
Composition (SiC:Cu)	2	0.011	10.44%	0.011	0.005	0.48	0.677
Error	2	0.022	21.91%	0.022	0.011	—	—
Total	8	0.102	100.00%	—	—	—	—
B. TOPSIS							
Compaction load (ton)	2	0.034	13.58%	0.034	0.017	0.29	0.776
Current (A)	2	0.071	27.88%	0.071	0.035	0.59	0.628
Composition (SiC:Cu)	2	0.029	11.53%	0.029	0.015	0.25	0.803
Error	2	0.119	47.01%	0.119	0.059	—	—
Total	8	0.253	100.00%	—	—	—	—

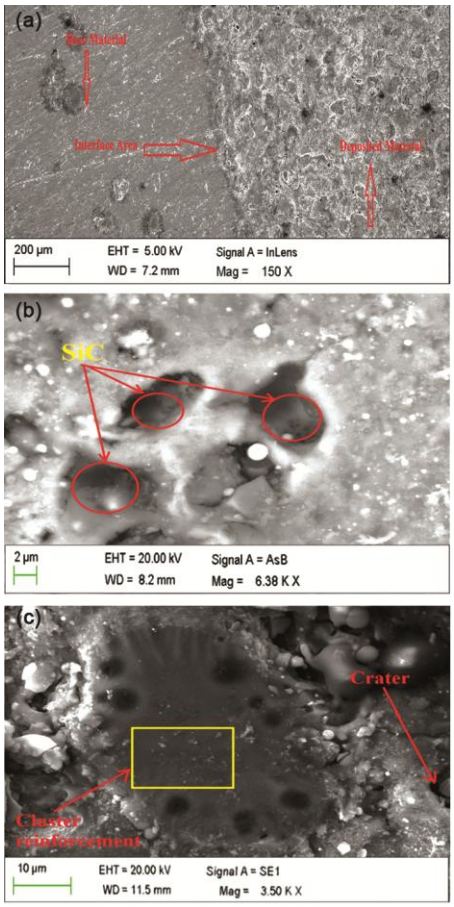

Fig. 3 — SEM image of the sample: (a) top surface after EDC; (b) at 5 ton, 6A and 50:50; and (c) at 5 ton, 2A and 30:70

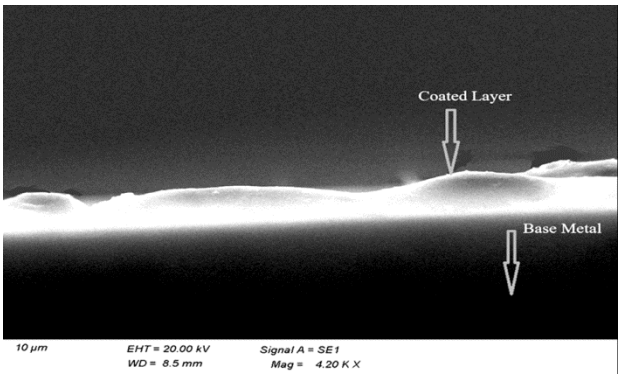

Fig. 4 — Layer thickness of a coated sample

over the work surface and an average layer thickness of 14.03 µm has been achieved as shown in Fig. 4.

Phase Analysis

X-ray diffraction (XRD) analysis serves a key purpose in identifying materials by examining their diffraction patterns and determining their phases. In the context of the EDC process, XRD analysis was employed to identify phase formations resulting from

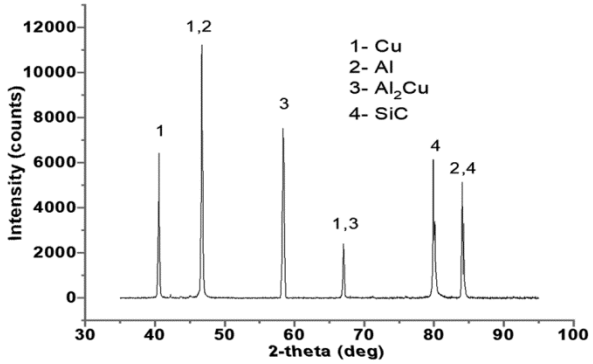

Fig. 5 — XRD plot of a coated sample

chemical reactions. The X'Pert High Score Plus stands out as a comprehensive tool for analyzing full powder patterns. It seamlessly integrates phase identification, crystallographic analysis, and cluster analysis serving various common applications in powder diffraction.

The X-ray data were scrutinized using the aforementioned tool to ascertain diffraction phases and peaks for the coated sample within the diffraction angle range of 30° to 90°, as depicted in Fig. 5. The analysis revealed the presence of various compounds and elements, including Al, Cu, SiC, and Al_2Cu, in the coated sample. The formation of Al_2Cu, can be attributed to the interaction between the tool material and the dielectric fluid of EDM. The XRD analysis (Fig. 5) clearly indicates the existence of intermetallic compound phases such as Al_2Cu and SiC, which confirms the migration of tool material to the work piece surface.

Conclusions

The EDC process with SiC-Cu P/M tool was successfully employed in this work to deposit a uniform film of SiC on the surface of Al-7075 substrate. The EDC responses (MDR, TWR and SR) were optimized using Taguchi, GRA and TOPSIS optimization techniques. Both GRA and TOPSIS methods identified the optimal process variables as compaction load of 5 ton, composition of 50:50 and current of 6 A. The response values from the optimal set, in comparison to the initial run in the experimentation, showed improvements of 0.2175 and 0.5241 using GRA and TOPSIS, respectively. From ANOVA, compaction load and current evolved as the most significant parameters for GRA and TOPSIS, respectively. The SEM and XRD analyses confirmed the presence of SiC on Al-7075 surface, migrated from the P/M tool electrode. These findings and hypotheses can be useful for industries looking to conduct further research on surface modification.

References

1 Chen Y F, Chow H M, Lin Y C & Lin C T, Surface modification using semi-sintered electrodes on electrical discharge machining, *Int J Adv Manuf Technol*, **36(5–6)** (2008) 490–500, https://doi.org/10.1007/s00170-006-0859-x.

2 Suzuki T & Kobayashi S, Mechanisms of TiC layer formation on high speed steel by a single pulse in electrical discharge machining, *Electrochim Acta*, **114** (2013) 844–850, https://doi.org/10.1016/j.electacta.2013.10.041.

3 Gill A S & Kumar S, Investigation of micro-hardness in electrical discharge alloying of EN31 tool steel with Cu–W powder metallurgy electrode, *Arab J Sci Eng*, **43(3)** (2018) 1499–1510, https://doi.org/10.1007/s13369-017-2960-x.

4 Gong S, He X, Wang Y & Wang Z, Material removal mechanisms, processing characteristics and surface analysis of C_f-ZrB_2-SiC in micro-EDM, *Ceram Int*, **48(20)** (2022) 30164–30175, https://doi.org/10.1016/j.ceramint.2022.06.289.

5 Yue X, Li Q & Yang X, Influence of thermal stress on material removal of C_f_SiC composite in EDM, *Ceram Int*, **46(6)** (2020) 7998–8009, https://doi.org/10.1016/j.ceramint.2019.12.022.

6 Jahan M P, *Electrical Discharge Machining (EDM) Types, Technologies and Applications* (Nova Science Publishers, New York) 2015.

7 Selvarajan L, Rajavel R, Venkataramanan K & Srinivasan V P, Experimental investigation on surface morphology and recasting layer of Si_3N_4-TiN composites machined by die-sinking and rotary EDM, *Ceram Int*, **49(5)** (2023) 8487–8501, https://doi.org/10.1016/j.ceramint.2022.11.011.

8 Kumar R, Pandey A & Sharma P, Electrical discharge machining of inconel 718 using cryo-processed rotary Cu-electrode, *J Sci Ind Res (India)*, **79(8)** (2020) 691–695, https://doi.org/10.56042/jsir.v79i8.41411.

9 Ho K H & Newman S T, State of the art electrical discharge machining (EDM), *Int J Mach Tools Manuf*, **43(13)** (2003) 1287–1300, https://doi.org/10.1016/S0890-6955(03)00162-7.

10 Tsai H, Yan B & Huang F, EDM performance of Cr/Cu-based composite electrodes, *Int J Mach Tools Manuf*, **43(3)** (2003) 245–252, https://doi.org/10.1016/S0890-6955(02)00238-9.

11 Kumar S, Singh R, Singh T P & Sethi B L, Surface modification by electrical discharge machining: a review, *J Mater Process Technol*, **209(8)** (2009) 3675–3687, https://doi.org/10.1016/J.JMATPROTEC.2008.09.032.

12 Chakraborty S, Kar S, Dey V & Ghosh S K, The phenomenon of surface modification by electro-discharge coating process: a review, *Surf Rev Lett*, **25(1)** (2018) 1830003, https://doi.org/10.1142/S0218625X18300034.

13 Mussada E K & Patowari P K, Characterisation of layer deposited by electric discharge coating process, *Surf Eng*, **31(10)** (2015) 796–802, https://doi.org/10.1179/1743294415Y.0000000048.

14 Samuel M P & Philip P K, Power metallurgy tool electrodes for electrical discharge machining, *Int J Mach Tools Manuf*, **37(11)** (1997) 1625–1633, https://doi.org/10.1016/S0890-6955(97)00006-0.

15 Das A & Misra J P, Experimental investigation on surface modification of aluminum by electric discharge coating process using TiC/Cu green compact tool-electrode, *Mach Sci Technol*, **16(4)** (2012) 601–623, https://doi.org/10.1080/10910344.2012.731951.

16 Chakraborty S, Kar S, Dey V & Ghosh S K, Optimization and surface modification of Al-6351 alloy using SiC–Cu green compact electrode by electro discharge coating process, *Surf Rev Lett*, **24(1)** (2017) 1750007, https://doi.org/10.1142/S0218625X1750007X.

17 Chakraborty S, Kar S, Dey V & Ghosh S K, Multi attribute decision making for determining optimum process parameter in EDC with Si and Cu mixed powder green compact electrodes, *J Sci Ind Res*, **77(4)** (2018) 229–236.

18 Patowari P K, Mishra U K, Saha P & Mishra P K, Surface integrity of C-40 steel processed with WC-Cu powder metallurgy green compact tools in EDM, *Mater Manuf Process*, **26(5)** (2011) 668–676, https://doi.org/10.1080/10426914.2010.512652.

19 Gill A S & Kumar S, Surface roughness and microhardness evaluation for EDM with Cu–Mn powder metallurgy tool, *Mater Manuf Process*, **31(4)** (2016) 514–521, https://doi.org/10.1080/10426914.2015.1070412.

20 Gülcan O, Uslan İ, Usta Y & Çoğun C, Performance and surface alloying characteristics of Cu–Cr and Cu–Mo powder metal tool electrodes in electrical discharge machining, *Mach Sci Technol*, **20(4)** (2016) 523–546, https://doi.org/10.1080/10910344.2016.1191031.

21 Kumar P M, Sivakumar K & Jayakumar N, Surface modification on OHNS steel using Cu-CrB_2 green compact electrode in EDM, *Mater Today Proc*, **5(9)** (2018) 17389–17395, https://doi.org/10.1016/j.matpr.2018.04.152.

22 Chundru V R, Koona R & Pujari S R, Surface modification of Ti6Al4V alloy using EDMed electrode made with nano- and micron-sized TiC/Cu powder particles, *Arab J Sci Eng*, **44(2)** (2019) 1425–1436, https://doi.org/10.1007/s13369-018-3561-z.

23 Mazarbhuiya R M & Rahang M, Reverse EDM process for pattern generation using powder metallurgical green compact tool, *Mater Manuf Process*, **35(15)** (2020) 1741–1748, https://doi.org/10.1080/10426914.2020.1802036.

24 Sarmah A, Kar S & Patowari P K, Surface modification of aluminum with green compact powder metallurgy inconel-aluminum tool in EDM, *Mater Manuf Process*, **35(10)** (2020) 1104–1112, https://doi.org/10.1080/10426914.2020.1765253.

25 Meel R, Singh V, Katyal P & Gupta M, Optimization of process parameters of micro-EDD/EDM for magnesium alloy using Taguchi based GRA and TOPSIS method, *Mater Today Proc*, **51** (2021) 269–275, https://doi.org/10.1016/j.matpr.2021.05.287.

26 Manivannan R & Kumar M P, Multi-response optimization of micro-EDM process parameters on AISI304 steel using TOPSIS, *J Mech Sci Technol*, **30(1)** (2016) 137–144, https://doi.org/10.1007/s12206-015-1217-4.

27 Srinivasan V P, Palani P K & Balamurugan S, Experimental investigation on EDM of Si_3N_4–TiN using grey relational analysis coupled with teaching-learning-based optimization algorithm, *Ceram Int*, **47(13)** (2021) 19153–19168, https://doi.org/10.1016/j.ceramint.2021.03.262.

28 Baroi B K, Kar S & Patowari P K, Electric discharge machining of titanium grade 2 alloy and its parametric study, *Mater Today Proc*, **5(2)** (2018) 5004–5011, https://doi.org/10.1016/J.MATPR.2017.12.078.

29 Singh A K, Patowari P K & Chandrasekaran M, Experimental study on drilling micro-hole through

micro-EDM and optimization of multiple performance characteristics, *J Brazilian Soc Mech Sci Eng*, **42(10)** (2020) 506, https://doi.org/10.1007/S40430-020-02595-w.

30 Kar S, Chakraborty S, Dey V & Ghosh S K, Optimization of surface roughness parameters of Al-6351 alloy in EDC process: a Taguchi coupled fuzzy logic approach, *J Inst Eng Ser C*, **98(5)** (2017) 607–618, https://doi.org/10.1007/s40032-016-0297-y.

31 Roy R K, *Design of Experiments Using The Taguchi Approach: 16 Steps to Product and Process Improvement* (Wiley, New York) 2001.

32 Srinivasan L, Chand K M, Kannan T D B, Sathiya P & Biju S, Application of GRA and TOPSIS optimization techniques in GTA welding of 15CDV6 aerospace material, *Trans Indian Inst Met*, **71(2)** (2018) 373–382, https://doi.org/10.1007/S12666-017-1166-y.